MolEV: Auto-Molecular Generation Framework for Inhibitor Evolution of POLQ Enzyme

1st Zekai Shen
Faculty of Pharmacy
China Pharmaceutical University
NanJing, China
szkchris@sina.com

2nd Zexuan Wei
Faculty of Pharmacy
China Pharmaceutical University
NanJing, China
MoriyaSuwako2524@163.com

3rd Xvjian Wang
College of Life Sciences and Technology
China Pharmaceutical University
NanJing, China
wang.xvjian.2021@uni.strath.ac.uk

4th Lingyue Zhao
Faculty of Pharmacy
China Pharmaceutical University
NanJing, China
zhaolingyue_sz@outlook.com

5th Tianle Xiong
Faculty of Pharmacy
China Pharmaceutical University
NanJing, China
xtlltx1109@163.com

6th Zeyu Cai
Faculty of Pharmacy
China Pharmaceutical University
NanJing, China
2020200300@stu.cpu.edu.cn

7th Yuling Cao
Faculty of Pharmacy
China Pharmaceutical University
NanJing, China
2020210750@stu.cpu.edu.cn

8th Haodong Liu
Faculty of Pharmacy
China Pharmaceutical University
NanJing, China
haodonliu@foxmail.com

9th YueZhang
Faculty of Pharmacy
China Pharmaceutical University
NanJing, China
2020192236@stu.cpu.edu.cn

10th Tianchang Xia
Faculty of Pharmacy
China Pharmaceutical University
NanJing, China
492691032@qq.com

11th YuanMu
Faculty of Pharmacy
China Pharmaceutical University
NanJing, China
muyuan2482@163.com

12th Hongjie Qian
Strathclyde Institute of Pharmacy
China Pharmaceutical University
NanJing, China
hongjie.qian.2019@uni.strath.ac.uk

***Abstract*—DNA polymerase enzyme (Pol) is an attractive synthetic lethal target in drug discovery field, which is expected to have a significant impact on breast and ovarian cancers containing BRCA mutation alleles. Here, we described a small molecule inhibitor screening framework for POLQ enzyme targets based on molecular geometry information (protein mesh). Since the 1D SMILES sequence ignores molecular structure features, it is impossible to learn smooth molecular embeddings; 2D molecular maps are easier to express molecules more intuitively, but for similar molecular diagrams, they tend to have different 3D structures and molecular properties. The feature coding of 1D and 2D limits feature discovery to predefined molecular 1D or 2D structures, eliminating the ability to discover any features that are one of the most critical factors in determining molecular properties and understanding how they work in the physical world, and capturing three-dimensional spatial structural features is essential for molecular generation. Before that, we also designed a model to predict the binding sites of proteins to facilitate the subsequent molecular sampling and evolution process. After structural optimization of the generated molecules, we calculated the relatively free energy perturbation (FEP) of ligand molecules under the condition of high molecular shape similarity after large-scale molecular screening (ledock), and calculated the binding free energy of MMGBSA under the condition of low molecular similarity, So as to screen out a relatively high-quality small molecule inhibitors.**

***Index Terms*—FEP, MMGBSA, evolution, geometry, mesh**

I. Introduction

DNA double-strand breaks (DSBs) during DNA replication or due to exogenous insults, including irradiation and chemotherapy, are highly deleterious lesions that can induce genome instability and lead to cell death. Mammalian cells have evolved multiple pathways to repair DSBs. DNA polymerase theta (pol) is a key component of the alternative end joining (ALT EJ) pathway, also known as the microhomology mediated end joining (MMEJ) pathway, involved in DNA double strand break repair. MMEJ is another repair pathway of the cell in addition to non homologous end joining (NHEJ) and homologous recombination (HR). The repair of MMEJ is driven by the annealing of microhomologous sequences flanking the DNA ends and was initially thought to function as a backup pathway for gene repair, and as research progressed, it was also found that MMEJ was not a backup repair mechanism. When DNA end resection occurs, in the presence of BRCA2, BRCA2 not only recruits the recombinase Rad51 to DSBs to promote HR but also inhibits repair pathways such as ALT NHEJ.

Pol θ [1] inhibitors is an intriguing drug target. It is still unclear which domain, helicase-like (hld), polymerase (pol),

or the central unstructured region, is the ideal target for drug development. Recently, most of the published small molecule inhibitors have inhibitory effects on the helicase domain, which is a good phenomenon, but the number of existing inhibitors is relatively small. In order to accelerate the discovery of small molecule inhibitors of DNA polymerase theta, we propose a geometry based VAE model (you can visit this link:*https://github.com/CondaPereira/MolEV*), hoping to find more effective molecule inhibitors, which will pave the way for fragment molecular design. Since the specific binding sites of small molecule inhibitors have not been published in the relevant document, we proposed a protein binding pocket prediction model (Presite) mainly based on ligand site, L-J potential and coulomb force.

II. Experiment results

A. Protein optimization and ligand preparation

Before extracting the structural information features of protein and inhibitors, we needed to optimize the molecular structure, so as to improve the reliability of the extracted molecular 3D structural information. Otherwise, errors and inaccurate results will be reported in the subsequent simulation process. For the structural optimization of polymerase theta enzyme, we found that it lacks many loops, so it is important to repair the loop region of the protein. After sequence observation, we found that most of the missing loops are within the range of 5-10. Therefore, after the rough structure containing loops is repaired by the cyclic coordinate center (CCD) [2], we further rationally optimize the generated loop structure through the closed-loop algorithm KIC, Set a loop with four node amino acids, and then cut it from the middle node to form a cut. Then, use the fastelax module in rosetta [3] to eliminate the unreasonable conformation in the protein crystal structure and compare the energy changes between multiple structures. Among them, we search for the optimal conformation at the local energy barrier of a given three-dimensional structure through five iterations (single protein) of amino acid side chain rearrangement and energy minimization calculation, The side chain can enter a new energy minimum point. After that, the $\boldsymbol{clique}$ algorithm is used to cluster the 600 protein structures screened, so as to screen out a more reasonable conformation, after that, foldx was used to conduct annealing optimization and self mutation optimization for the obtained structure in the environment with ionic strength of 0.05 and PH=7. Finally, pdb4amber tool in amber22 was used with reasonable Hydrogens, so far, the protein structure optimization was completely completed, as shown in the following Fig.1:

After optimizing the protein, we need to prepare the ligand file for the subsequent extraction of structural information. Because we have generated about 300 small molecules with high druglike properties for the POLQ target according to our model, due to the computational power, we used the $\boldsymbol{GFN2-xtb}$ [4] algorithm to optimize these structures separately at the beginning. After hydrogenated docking, The virtual screened molecules are then optimized and calculated

Fig. 1. the final optimized DNA polymerase theta structure

using the $\boldsymbol{B3LYP/B97-3c}$ [5] in combination with the $\boldsymbol{def2-TZVP}$ basis set. At the same time, the $\boldsymbol{RESP2}$ [6] charge of the molecules is calculated using Multiwfn [11], which further replace the $\boldsymbol{am1-bcc}$ charge used in molecular dynamics simulation. Because the RESP2 charge can greatly reduce the following two problems in using $\boldsymbol{MK/CHELPG}$ charges, (1) the results are highly conformational, (2) Inaccurate fitting of embedded atomic charge.

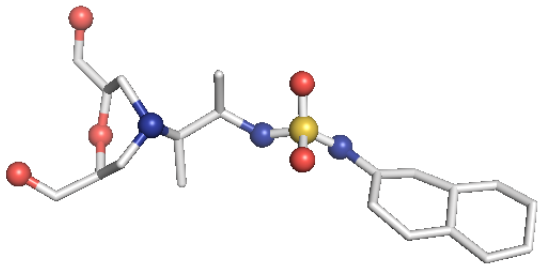

Fig. 2. The optimized molecule (example) calculated by ORCA with B3LYP/def2-TZVP level

The structures in this model have all been optimized. After checking the protein structure according to the tleap module in amber22 [7][8] , it is found that there is no problem, and no virtual frequency (vibration) is found in the output files of the xtb and ORCA [9] .

B. Construction and principle of the Model (Presite)

Before building the molecular generative model, we built the neural network prestige with the CNN as the main body of predicted protein binding pockets, and its main architecture is described below. A four-channel grid protein descriptor is constructed based on ligand site (ligsite), L-J potential, and Coulomb force, which can be used for protein binding site prediction. By using $12 \times 12 \times 12$sampling to classify and cluster the blocks, the binding sites of the proteins are

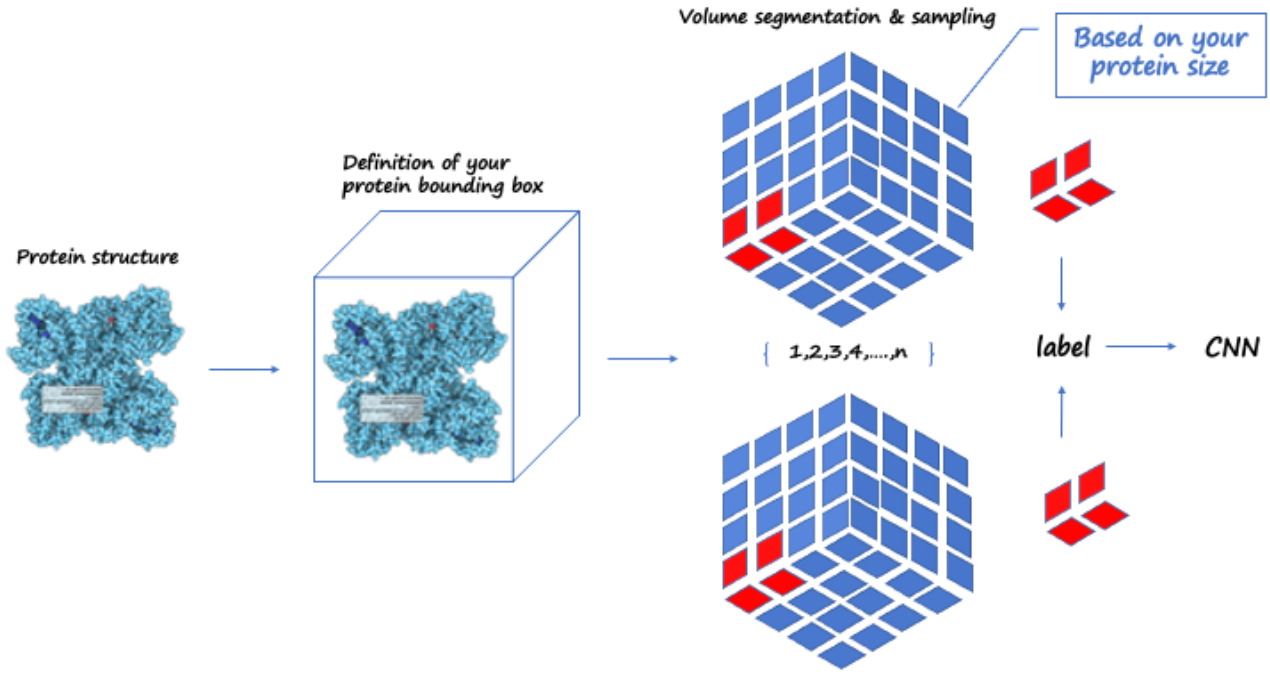

Fig. 3. Framework about predicting the protein pocket

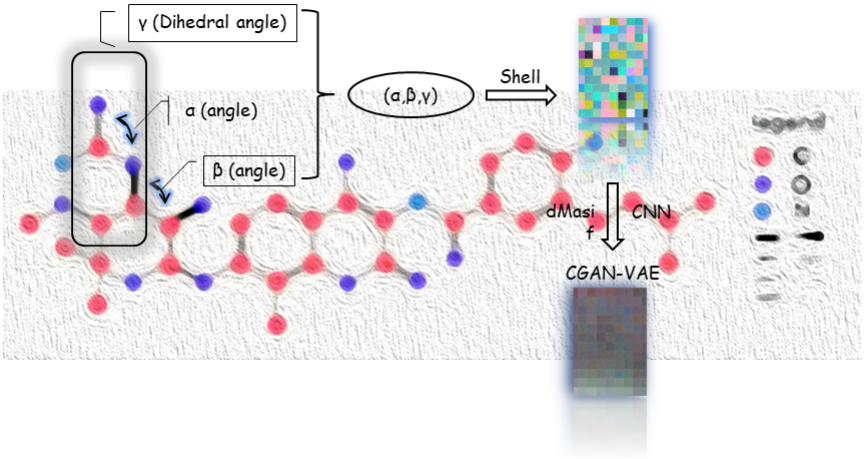

Fig. 4. Main part and details of our MolEV Model

finally determined. At the same time, in order to obtain protein feature, the pdbqt files of the protein should be included in the dataset, and we suggest that you can get these files through openbabel or ADFRsuites. The detailed processing is shown in the figure3 below and our training dataset is based on the ***scPDB*** [10] database.

We define a geometric vector MLP as a GVP block followed by a GVL block, denoted as G_m. The frontier predictor takes the features of atom i as input and utilizes one MLP layer to predict the probability of being a frontier p_f as follows:

$$(p_f, \vec{P}_f) = G_m^f(v^{\cdot}, \vec{v}_i) \tag{1}$$

C. Construction and principle of the model (MolEV)

In the generation of the molecule, we divided it mainly into two parts called molgraph and prograph, respectively, in Molgraph, we extracted the dihedral angle of the molecule With two geometric angles α, β, we set four atoms of the molecule into one set (α, β, γ) arrays and mapped to RGB triple primaries:

$$\sum_{i=1}^{n}(\alpha_i, \beta_i, \gamma_i) \longmapsto \sum_{i=1}^{n}(R_i, G_i, B_i) \tag{2}$$

After this, the (α, β, γ) array is transformed into a picture

and the CVAE_GAN neural network model is constructed for data training to obtain a new picture, where C represents the information about the geometry of the protein, is a restriction for molecular generation, after which the picture is transposed to obtain a suitable fit for a specific protein structure or target pair small molecule inhibitors with ligands.

In order to make our extracted molecular arrays of some physical significance, we propose $\boldsymbol{Besselfunctions}$ applicable to biological molecular geometry systems as follows

$$\psi(\alpha,\beta,\gamma) = jl(\frac{Bl_n}{c}\alpha)Y_l^m(\beta,\gamma) \tag{3}$$

Where $jl()$ is the spherical Bessel function of order l, $Y_l^m$is the spherical harmonic function, C represents cutoff, and βl_n is the N-Solution of the Bessel function of order . In this way, the triple (α,β,γ) can represent the relative position of any atom in a 3D molecular graph through a spherical message passing network, and a more accurate and physically meaningful representation can be generated by combining the positional information in the spherical coordinates, which avoids the problem of missing physical meaning of most molecular descriptors generated through machine learning. Our main model ($\boldsymbol{MolEV}$) details are shown in Figure4.

For the part of $\boldsymbol{Prograph}$, we used this year's improved framework dmasif for feature extraction from the protein surface and input the extracted geometry information into our model as a restrictive condition . Based on the eMolFrag repository, we develop a classical way to recombine the previously cleaved groups to generate new small molecules from mol2 structure format and make some fixes for the previous bug in eMolFrag to make it work more properly.

D. Model training

In the training stage, we randomly mask atoms of molecules and train the model to recover the masked atoms. Specifically, for each pocket-ligand pair, we sample a mask ratio from the uniform distribution U[0, 1] and mask corresponding number of molecular atoms. The remaining molecular atoms that have valence bonds to the masked atoms are defined as frontiers. Then the position predictor and the element-and-bond predictor try to recover the masked atoms that have valence bonds to the frontiers by predicting their positions towards corresponding frontiers, the element types and the bonds with remaining molecular atoms. If all molecular atoms are masked, the frontiers are defined as protein atoms that have masked atoms within 4A and the masked atoms around the frontiers are to be recovered. For the element type prediction, we add one more element type representing Nothing at the query position. During the training process, we sample not only the positions of masked atoms for element type predictions but also negative positions from the ambient space and assign their labels as Nothing.

The loss of the frontier prediction, Φ_f, is the binary cross entropy loss of predicted frontiers. The loss of the position predictor, Φ_p, is the negative log likelihood of the masked atom positions. For the element type and bond type prediction, we used cross entropy losses for the classification, denoted as Φ_e and Φ_b respectively. The overall loss function is the summation of the above four loss functions:

$$\Phi = \Phi_f + \Phi_p + \Phi_e + \Phi_b \tag{4}$$

E. Molcular Dynamic Simulation (MMGBSA And FEP)

After a certain amount of sampling, we first use ledock_ Omega [12] to obtain a series of molecular conformations through mass molecular docking and related property evaluation, including drug like properties, vdw, hbond quantity, etc. Some results are preseneted as Figure5 follows:

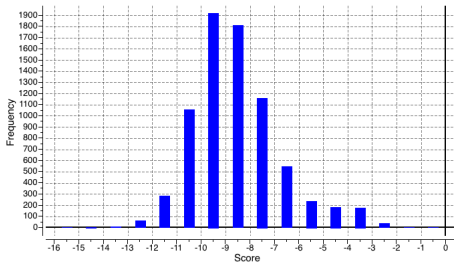

Fig. 5. General docking score range which is screened by ledock

We subsequently conducted the hydrated docking after the previous round of primary screening, that is, the incorporation of explicit water model in the process of docking, improved the precision of docking, because this docking relies on reasonable protein conformation with correct molecular structure, reasonable molecular optimization steps before is highly necessary, after passing the less selections, We selected three molecules with extremely close molecular structures for the 5ns FEP calculations (constrained by computational conditions) and then verified the molecular activities (obtaining the relative free energy between ligand molecules) and performed MMGBSA binding free energy calculations after finally picking the optimal result molecule.

The results showed that the relative free energies of molecular conversion of ART558 and ART615 into ART4215 molecules were -0.2kal/mol and -0.4 kcal/mol, respectively, well demonstrating the stronger activity of ART4215 relative to the other two molecules, and according to the display of the following three graphs, it can be concluded that our simulation reached the level of convergence, After that we subjected the complex of art4215 with POLQ enzyme for up to 200 ns simulation and took the last two thousand frames in the trajectory to calculate the mmgbsa binding free energy, which resulted -27.3786 kcal/mol. The relative RMSD curves generated during the above simulations are provided in thesupplementary files.

F. Model Results and Evalution

Our model is to generate molecules in the pocket after a good protein pocket is determined, so the process of molecular docking can be omitted to some extent, the most powerful demonstration is shown in Fig. 7. As shown in Figure7, using

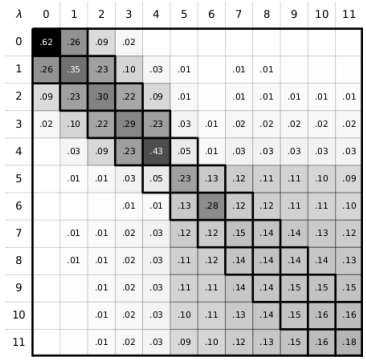

Fig. 6. Overlap matrix of free energy perturbation calculation

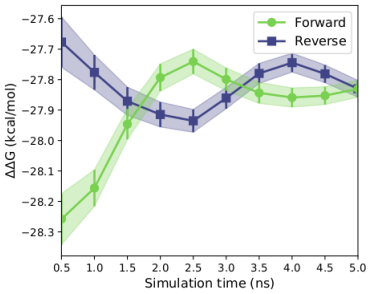

Fig. 7. Overlap matrix of free energy perturbation calculation

the hydrated docking of vina, the obtained conformations and models generated by the molecules do not differ much with RMSD ranging from 0.05 to 0.15, but the verification of scoring function is missing, experimentally, For reasons of time there is no way to implement relevant synthetic experiments and in vitro drug trials and there has not been a certain comparison and validation with other VAE models, such as the JT-VAE and so on.

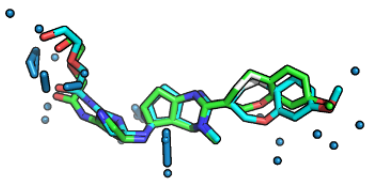

Fig. 8. RMSD deviation between gernerated molecule in the pocket and hydrated docking by vina

G. Conclusion and table

In general, we calculated the druglike fraction and novelty of the 400 molecules generated by the model, and found that the molecules with excellent druglike properties generated by MolEV often have good novelty. We introduced geometric structure features in the model construction, which also improved the performance of the model. At the same time, when we use metalloenzymes to generate molecules, we often cannot get good structures, The resulting conformation tends to be biased towards the generation of phosphate ions, or even the generation of unstable sulfone hydrolysates. Therefore, in the presence of metal ions, our model is not applicable, and there are significant defects, which also need to be improved. Furthermore, our training set does not use PDBbind, because we found that PDBbind dataset is used in the process of molecular generation, The conformation of the molecule is strongly dependent on the structure of the ligand molecule contained in PDBbind itself. The molecules generated are relatively similar, and there is still a big gap with our expected goal, namely novelty. The following table shows whether some of the molecules (inhibitors) generated for the POLQ target can really play the role of inhibitors, which needs to be verified by synthesis and activity in subsequent experiments.

Molecule	Score	VDW	Hbond
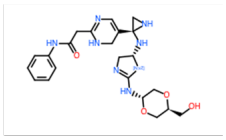	-5.676	82.44	-29.54
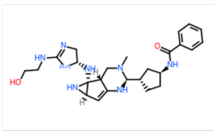	-8.408	-32.16	-33.73
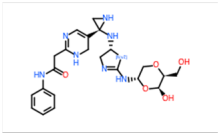	-8.779	-41.48	-32.56
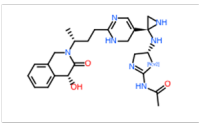	-9.923	-38.6	-39.56
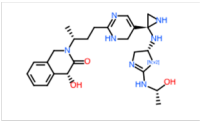	-8.091	41.36	-20.47
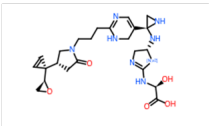	-8.727	-36.76	-22.16
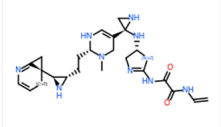	-8.311	-40.21	-15.77

Fig. 9. Some molecule generated by our models and their basic property

H. Software

All the experiments are conducted on Ubuntu Linux with RTX3090Ti GPUs. The codes are implemented in Python 3.8 mainly with Pytorch 1.9.0 and our codes are uploaded as Supplementary Material.

ACKNOWLEDGMENT

With our mostgratitude, We thank YanZhe Zhang from Westlake University provided us a lot of inspiration and suggestions in extracting protein structure feature module. We thank Dr. Yadong Chen from China Pharmaceutical University provided us certain server equipment and technical support.

Finally, The International Directed Evolution Competition-inspired us to explore this field. We thank iDEC for providing such an good opportunity.

REFERENCES

[1] Newman JA, Cooper CDO, Aitkenhead H, Gileadi O. Structure of the Helicase Domain of DNA Polymerase Theta Reveals a Possible Role in the Microhomology-Mediated End-Joining Pathway. Structure. 2015 Dec 1;23(12):2319-2330. doi: 10.1016/j.str.2015.10.014. PMID: 26636256; PMCID: PMC4671958.

[2] Kaufmann, K.W., et al., Practically useful: what the Rosetta protein modeling suite can do for you. Biochemistry, 2010. 49(14): p. 2987-98.

[3] Leaver-Fay, A., et al., ROSETTA3: an object-oriented software suite for the simulation and design of macromolecules. Methods in enzymology, 2011. 487: p. 545.

[4] GFN2-xTB: Bannwarth, C.; Ehlert, S.; Grimme, S. GFN2-xTB—An Accurate and Broadly Parametrized Self-Consistent Tight-Binding Quantum Chemical Method with Multipole Electrostatics and Density-Dependent Dispersion Contributions J. Chem. Theory Comput. 2019, 15 (3), 1652–1671 DOI: 10.1021/acs.jctc.8b01176

[5] Tirado-Rives J, Jorgensen WL. Performance of B3LYP Density Functional Methods for a Large Set of Organic Molecules. J Chem Theory Comput. 2008 Feb;4(2):297-306. doi: 10.1021/ct700248k. PMID: 26620661.

[6] LU Tian, CHEN Fei-Wu. Comparison of Computational Methods for Atomic Charges[J]. Acta Phys. -Chim. Sin., 2012, 28(01): 1-18.

[7] D.A. Case, T.E. Cheatham, III, T. Darden, H. Gohlke, R. Luo, K.M. Merz, Jr., A. Onufriev, C. Simmerling, B. Wang and R. Woods. The Amber biomolecular simulation programs. J. Computat. Chem. 26, 1668-1688 (2005).

[8] R. Salomon-Ferrer, D.A. Case, R.C. Walker. An overview of the Amber biomolecular simulation package. WIREs Comput. Mol. Sci. 3, 198-210 (2013).

[9] Neese, F. (2012) The ORCA program system, Wiley Interdiscip. Rev.: Comput. Mol. Sci., 2, 73–78.Neese, F. (2017) Software update: the ORCA program system, version 4.0, Wiley Interdiscip. Rev.:Comput. Mol. Sci., 8, e1327.

[10] Jérémy Desaphy, Guillaume Bret, Didier Rognan, Esther Kellenberger, sc-PDB: a 3D-database of ligandable binding sites—10 years on, Nucleic Acids Research, Volume 43, Issue D1, 28 January 2015, Pages D399–D404, https://doi.org/10.1093/nar/gku928

[11] Tian Lu, Feiwu Chen, J. Comput. Chem., 33, 580-592 (2012).

[12] Phys. Chem. Chem. Phys., 2016,18, 12964-12975

III. ADDITIONAL MATERIAL

We also calculated some features, for example, Morgan fingerprint of our generated molecules, RMSD curves, gromacs energy curves and so on, which are presented as follows:

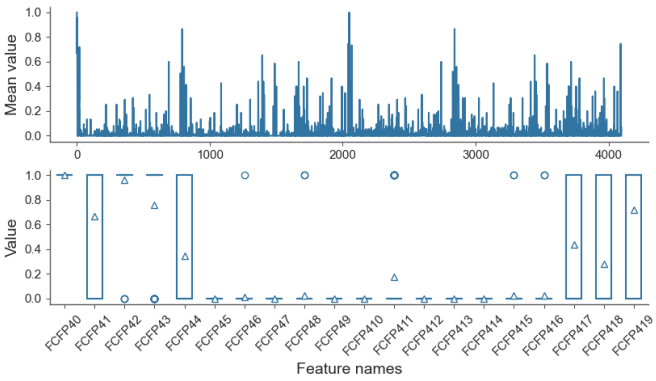

Fig. 10. Morgan characters of generated molecules

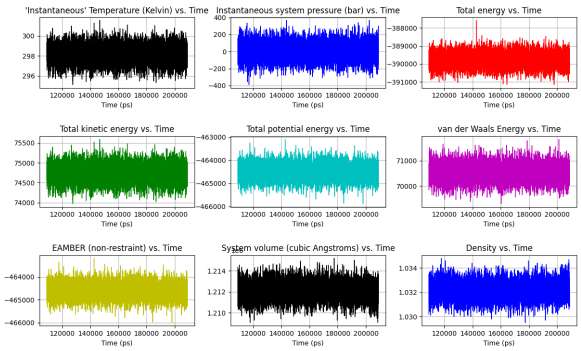

Fig. 11. System properties changes during the molcular dynamic simulation

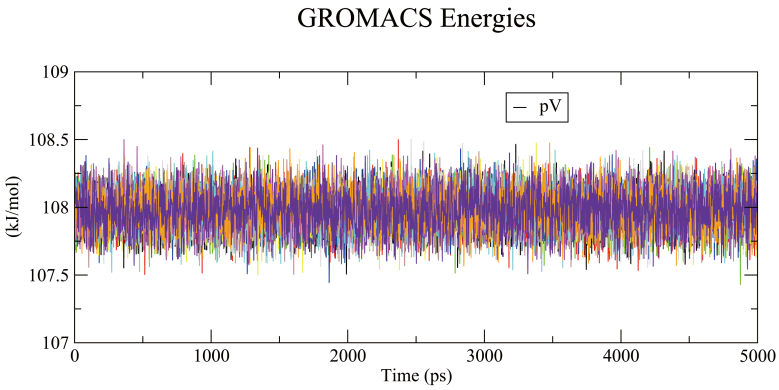

Fig. 12. 12 system energy changes during lambda calculation